ICAS 2021 SHANGHAI
International Council of the Aeronautical Sciences
32nd Congress of the International Council of the Aeronautical Sciences
September 6-10, 2021 Pudong Shangri-La, Shanghai, China

A TWO PHASES COUPLING FREE AND POROUS FLOW NUMERICAL SIMULATION METHOD OF LCM PROCESS

Chen Li[1,2], Cheng Chen[1,2], Limin Gao[1,2], Jifeng Xu[1]

[1]*Beijing Key Laboratory of Civil Aircraft Structures and Composite Materials, COMAC Beijing Aircraft Technology Research Institute, China, Beijing 102211, China*

[2]*Structure Integrity Department, COMAC Beijing Aircraft Technology Research Institute, China, Beijing 102211, China*

Abstract

In this research, a coupling CHNSD (Cahn-Hilliard-Navier-Stokes-Darcy) two-phase flow model is developed to simulate the Liquid composite molding (LCM) processes at multiple scales. A fiber reinforcement can be considered as a multi-scale porous media with large inter-tow pores and slight intra-tow pores. The Navier-Stokes equation is applied in the large inter-tow pores region, while two phase Darcy's law governs flow in the intra-tow pores considered as a porous medium. The refined "BJS" (Beavers-Joseph-Saffman) condition is included at the coupling interface condition to solve the two phase and two medium coupling problems. Flow flux, normal stress and velocity continuity are also taken into consideration at the interface. Transient resin flow front tracking is carried out by adopting the Cahn-Hilliard equation. Results and validation are presented to show the reliability of our model.

Keywords: Numerical simulation, Two phases flow, Liquid Composite Molding, Multi-scale

1. Introduction

LCM (Liquid Composite Molding) processes have various advantages such as low-cost production, and clean and high-efficiency composites manufacturing. In the typical LCM process, resin flows in dry fibrous reinforcement before curing. The filling of reinforcement is a crucial step which will have a significant and direct influence on the quality and mechanical properties of the final composite part. At the meso-scale, due to the intricate structure of the reinforcement, the resin flow during the impregnation can be considered as free surface flow between tows and porous flow inside tows. At the macro-scale, the flow inside the whole reinforcement can be regarded as a porous flow, while the flow between the wall of the mold and the reinforcement, or inside the flow-net, can be regarded as free surface flow.

Nowadays, the numerical simulation research on the LCM process mostly focus on the porous medium flow. There are few studies for the coupling free flow and porous flow especially in a two phase situation. However, in the actual process of LCM, both types of flows are included.

Hwang and Advani [1] developed a new method to solve the Stokes-Brinkman equation to figure out effective permeability of dual scale fibrous porous media based on this method. Blais et al. [2] proposed a Stokes-Darcy coupled flow model with low permeability of the porous media to simulate the infusion process at macro-scale. However, the Brinkman equation has so far only been applied to solve single-phase coupling problems. It is known that this equation will cause numerous problems in two-phase porous flow [3].

At the micro scale, Stokes equation can be used in the whole flow domain. When the scale is upgraded to meso or macro scales, Darcy's law is suitable to describe the porous flow. While, for the free flow domain, Navier-Stokes equation remains available. Nevertheless, the order of these two equations are different, and appropriate conditions should be developed on the interface. The

purpose of this study is to setting up a model using numerical methods to solve this coupling two-phase free flow and porous flow problem.
Based on literature studies [3, 4], the target of this research is to develop a coupling CHNSD (Cahn-Hilliard-Navier- Stokes-Darcy) two-phase flow model by numerical simulation of LCM processes [5]. In this model, the Navier-Stokes equation, which could be simplified by Stokes equation in most classical cases, is applied in the free flow region, while two phase Darcy's law works in the porous medium. The Cahn-Hilliard equation is adopted as the approach to track the transient resin flow front. The refined "BJS" (Beavers-Joseph-Saffman) condition is included at the coupling interface condition to solve the two phase and two medium problems. Flow flux, pressure and velocity continuity are also taken into consideration at the interface conditions to maintain the conversation of mass.

2. Construction of mathematical model

2.1 Governing equations in porous flow region

In the porous flow region, there is the continuity equation (1), Darcy's equation (2) and auxiliary equations (3) to determine saturation and pressure at the interphases.

$$\varepsilon \frac{\partial(\rho_f S_f)}{\partial t} + \nabla \cdot (\rho_f \boldsymbol{u_{pf}}) = \rho_f q_f, f \ = \ r\ (\text{resin}), a\ (\text{air}) \tag{1}$$

Where ε is the dimensionless porosity of the porous preform; ρ_f is the density of the p-phase fluid; Sf is the saturation of f-phase fluid; q_f is the source/sink term of p-phase fluid and $\boldsymbol{u_{pf}}$ is the Darcy's velocity which can be achieved by solving the Darcy's law by considering the relative permeability:

$$u_{pf} = -\frac{\boldsymbol{K_p} k_r}{\mu_p} \nabla p_{pf}, f \ = \ r, a \tag{2}$$

Where $\boldsymbol{K_p}$ is the absolute permeability tensor of the porous medium. Hence, intra tow domain, the arrangement of the fiber in horizontal and vertical directions are the same of a transverse section. k_r denotes the relative permeability $0 \leq k_r(S_r) \leq 1$; p_{pf} is the pressure of p-phase fluid in porous medium and μ_p is the viscosity of p-phase. Other auxiliary equations include relationship of saturation and capillary pressure are listed below in equation (3).

$$S_r + S_a = 1, P_{pc}(S_e) = P_{pa} - P_{pr} \tag{3}$$

Where P_{pc} is the capillary pressure, P_{pa} and P_{pr} are the pressure of air and resin, respectively. Efficient saturation is defined as Se = Sr in this study. To realize and solve the governing equation in the porous medium, PDE (Partial Differential Equation) module in COMSOL Multiphysics is applied.

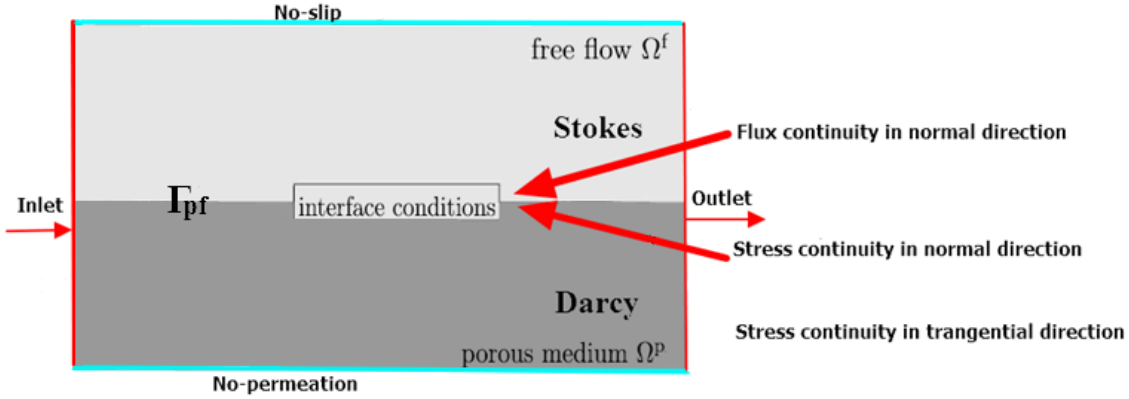

Figure 1 – Free flow and porous flow coupling interface condition of CHNSD method

The main difficulty lies on the coupling condition at the interface including continuity of normal flux, continuity of normal stress and the tangential stress jump condition.

2.2 Governing equations in free flow region

Flow front tracking equation: phase field method (Cahn-Hilliard equation in eq. 4):

$$\begin{cases} \Psi = -\nabla \cdot (\epsilon^2 \nabla \emptyset) + \emptyset(\emptyset^2 - 1) \\ \dfrac{\partial \emptyset}{\partial t} + \boldsymbol{u}_F \cdot \nabla \emptyset = \nabla \cdot \left(\dfrac{\gamma \beta}{\epsilon^2} \nabla \Psi \right) \end{cases} \tag{4}$$

Here Cahn-Hilliard equation is written in two equations. Ψ is an auxiliary phase field variable, ϵ is the thickness parameter of the interface, $\emptyset$ is the phase field variable and it is a dimensionless parameter, the value of $\emptyset$ is 1 in resin field while it is -1 in air field. $\boldsymbol{u}_F$ is the velocity of the free flow region. γ is the mobility, and β is the magnitude of the mixing energy.

Flow governing equation: (Navier-Stokes equation (5) and continuity equation (6)):

$$\rho(\boldsymbol{u}_F \cdot \nabla)\boldsymbol{u}_F = \nabla \cdot [-p_F \boldsymbol{I} + \mu(\nabla \boldsymbol{u}_F + (\nabla \boldsymbol{u}_F)^T)] + \boldsymbol{F} \tag{5}$$

$$\rho \nabla \cdot (\boldsymbol{u}_F) = 0 \tag{6}$$

where ρ[kg/m3], uF [m/s], pF [Pa], F [N], I are density, velocity in free flow region, pressure, volume force and unit matrix respectively. For our resin flow case, the fluid is Newtonian fluid and the Reynolds number is particularly low. Hence, inertial force can be ignored compared with the dominated viscous force. That is the reason why we use Stokes equation and not Navier-Stokes equation in the free flow domain.

2.3 Coupling condition on the interface of porous and free flow regions

Since the governing equations are different on porous and free flow regions, it is crucial to set up suitable coupling boundary condition to combine these two domains. For traditional BJS condition in some work, they considered that slip factor has nothing to do with the properties of the fluid but it is related to the geometric structure at the interface.

Continuity of normal flux

$$\boldsymbol{u}_F \cdot \boldsymbol{n}_{pf} = \boldsymbol{u}_{pf} \cdot \boldsymbol{n}_{pf} \tag{7}$$

Here $\boldsymbol{n}_{pf}$ is the normal vector.

Continuity of normal stress:

$$\boldsymbol{n}_{pf} \cdot \left[(-p_F \boldsymbol{I} + \boldsymbol{\tau})\boldsymbol{n}_{pf}\right] = -\left(\frac{1+\emptyset}{2} P_{pr} + \frac{1-\emptyset}{2} P_{pa}\right) = -\left(P_{pr} + \frac{1+\emptyset}{2} P_{pc}\right) \tag{8}$$

The tangential stress jump condition (Extended BJS boundary condition for two-phase flow)
Classical BJS condition is only valid for single-phase flow system in principle. When effective permeability and relative permeability are introduced, BJS condition can be extended to two phases situation as illustrated in equation (9):

$$\boldsymbol{t}_{PFi} \cdot [(-P_F \boldsymbol{I} + \boldsymbol{\tau})\boldsymbol{n}_{PF}] = -\boldsymbol{t}_{PFi} \cdot \frac{\mu \eta(S_r)}{\sqrt{K_p k_r(S_r)}} \boldsymbol{u}_F, \mathrm{i} = \{1, d-1, \mathrm{d} \leq 3\} \tag{9}$$

$\boldsymbol{t}_{PFi}$ is the tangent vector, d describes the dimension of RVE (Representative Elementary Volume). Relative permeability $k_r(S_r)$ = krr + kra is a function of saturation Sr, where relative permeability are defined as krr = Se, kra = 1-Se.Tangential jump interface condition is presented in Figure 1.

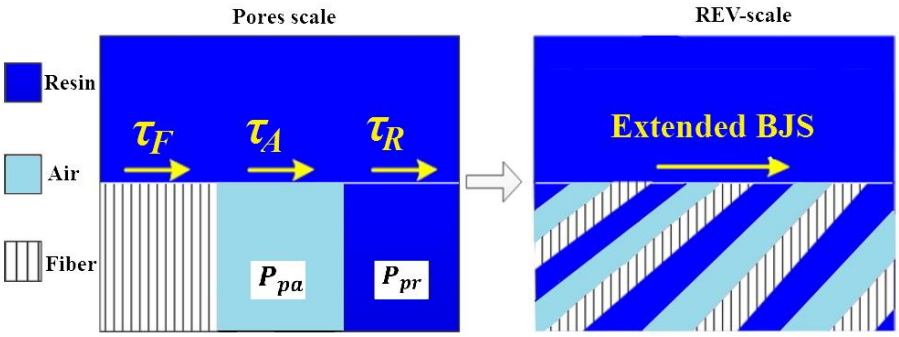

Figure 1: Tangential jump interface condition of free flow and porous flow

In COMSOL Multiphysics, partial differential equations are solved in "weak form". Weak form is an integrated form, it is suitable for solving FEM and non-linear problems since it requires low continuity from the integration variables. To set the extend BJS tangential jump interface condition (eq. 9) in COMSOL Multiphysics, weak form is applied as presented in equation (10).

$$\int_{\Gamma_{PF}} [(-P_F)\boldsymbol{I} + \tau \cdot n_{PF}] \cdot \tilde{u}_F dS = -\int_{\Gamma_{PF}} \left[P_P + \frac{\eta(Sr)\mu}{\sqrt{K_P}}(t_{PF} \cdot u_F)\right](n_{PF} \cdot \tilde{u}_F) dS \,, \mathrm{i} = \{1,2,d-1\} \qquad (10)$$

Here $\tilde{u}_F$ is the test function. The approach to solve the weak form equation is not the key point of this research, so the detailed process of calculability is not expressed here.

3. Comparison with Stokes method

In a real fiber tow, there are thousands or hundreds of fibers in it as shown in Figure 2(a), a 2D section of tows model is set up as presented in Figure 2(b). However, if the entire section is taken into consideration as the geometric model for numerical simulation, the calculation is too time-consuming to be realized. In the present work, one representative section in transverse direction presented in Figure 2(c) is extracted as the research region.

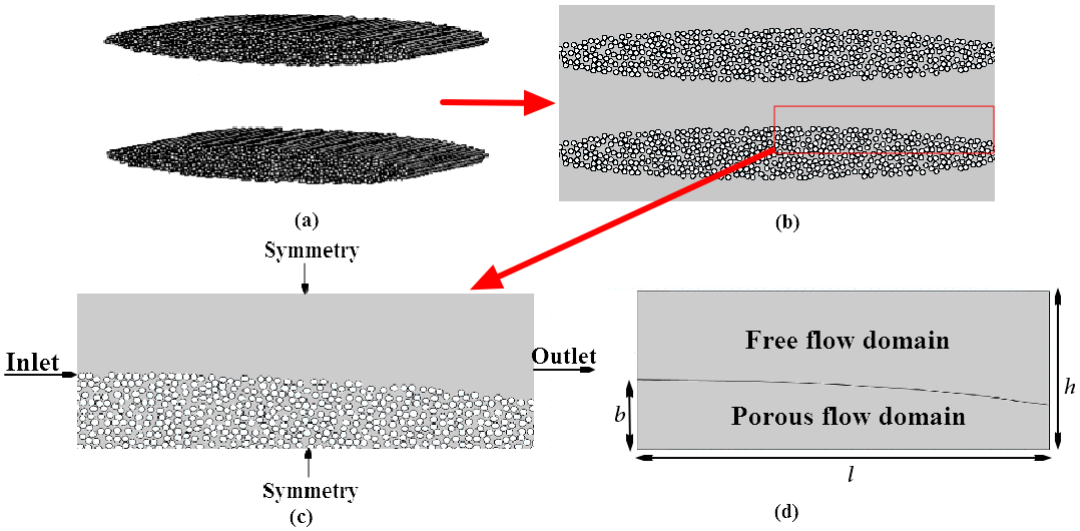

Figure 2: Geometric model definition and boundary condition

3.1 Boundary conditions and initial values

Inlet and outlet conditions are set on the left and right boundaries respectively. Symmetry conditions are set on the upper and lower boundaries as illustrated in Figure 2(c). Since for real resin and air, the difference between density and viscosity difference are very large. It is very difficult to carry out simulation if the real data is directly applied. Initial values and physical properties to input into the models for comparison are listed in the Table 1.

Table 1: Properties of the porous fibrous medium and fluids

Parameters	values
Porosity ε	0.5
Absolute permeability K_p	1×10^{-12} m^2

Density of resin ρ_r	1000 kg/m^3
Density of air ρ_a	10 kg/m^3
Viscosity of resin μ_r	0.1 Pa·s
Viscosity of air μ_a	0.01 Pa·s
Inlet pressure	1.001×10^5 Pa
Outlet pressure	1×10^5 Pa

3.2 Generation of the model applied Stokes equation

To set up the geometric model as illustrated in Figure 2(c) applied Stokes equation, a random fiber configuration approach developed in airticle [6-8] is applied to produce a realistic geometric fiber tow model.Here the porosity ε can be calculated by the expression in eq. 11.

$$\varepsilon = 1 - \frac{A_{fiber}}{A_{intra-tow}} \tag{11}$$

Where A_{fiber} is the area of fibers inside the tow region and $A_{intra-tow}$ is the area of entire tow.

3.3 Model used CHNSD method

For the coupling method, the classical Gebart's equation (12) is adopted to calculate the permeability in transverse direction of the porous tow since transverse flow model is only adopted in this study.

$$K_{t\perp} = \frac{16}{9\pi\sqrt{6}}\left(\sqrt{\frac{\pi}{2\sqrt{3}(1-\varepsilon)}} - 1\right)^{5/2} r_f^2 \tag{12}$$

Here the presented eq. 12 is in the form of maximum fiber fraction for the hexagonal fiber packing for transverse flow. Permeability estimation can be realized by solving this equation. For example, when he radius of a single fiber filament is defined as r_f = 7.8 μm, the transverse permeability estimated by eq. 12 is 10^{-12} m^2. In this paper, to set up the realistic geometric model in transverse direction (figure 1(c)), r_f = 7.8 μm is implemented to obtain the same permeability as input permeability value in the coupling CHNSD model.

FEM (Finite Element Method) is carried out by applying CFD software COMSOL Multiphysics to discretize the governing equations with free triangular mesh elements. For CHNSD coupling model, classical IMPES (Implicit Pressure, Explicit Saturation) approach [9] is applied to figure out the solution of pressure and saturation written in PDE (Partial Differential Equation) module in porous medium, coupling interface condition is realized by coding weak form.

3.4 Comparison and verification of flow front at different times

Flow front tracking by numerical methods are depicted in **Figure 3** with the geometric model size: 4mm in width and 1mm in vertical direction. In **Figure 3** (a), (c) and (e), Stokes equation is applied while CHNSD coupling method governs the flow in **Figure 3** (b), (d) and (f).

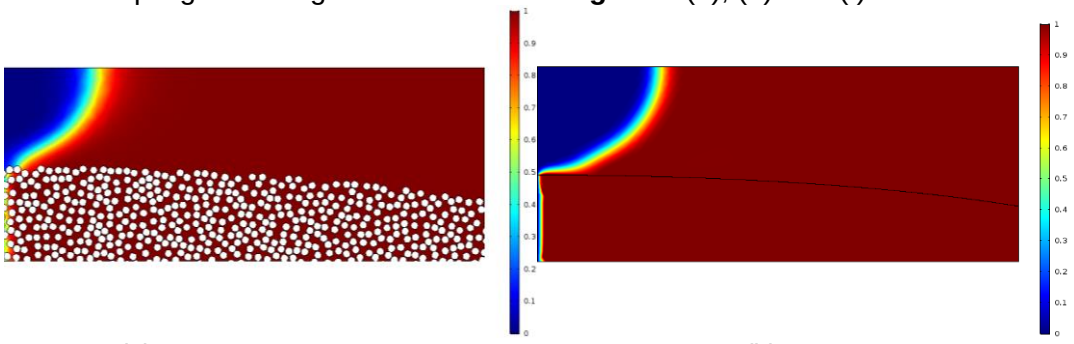

(a) (b)

t = 0.001s

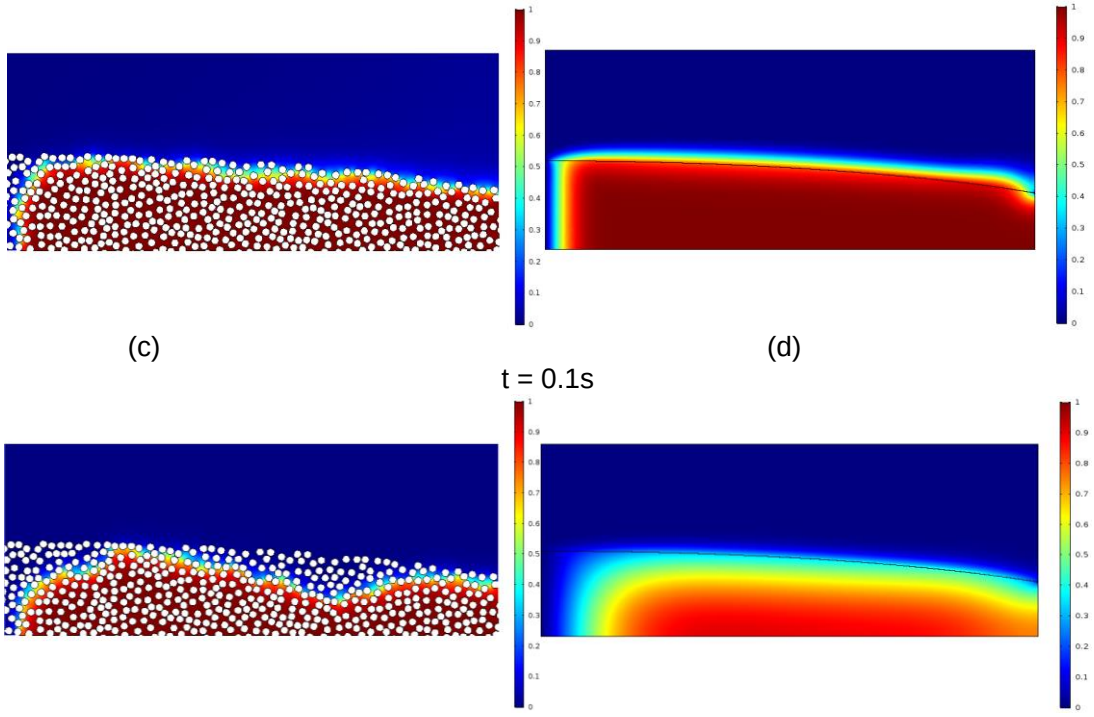

(c) (d)

t = 0.1s

(e) (f)

t = 1s

Figure 3: Comparison of flow front tracking process in two methods at different times

(a), (c)and (e): Stokes equation

(b), (d)and (f): CHNSD coupling method

Preferable agreement of transient saturation has been achieved at different time steps as illustrated in Figure 3. Resin flows much fast inter tow domain, then infuses into the tow step by step. Meanwhile, pressure continuity between free flow domain and porous medium is presented in Figure 4

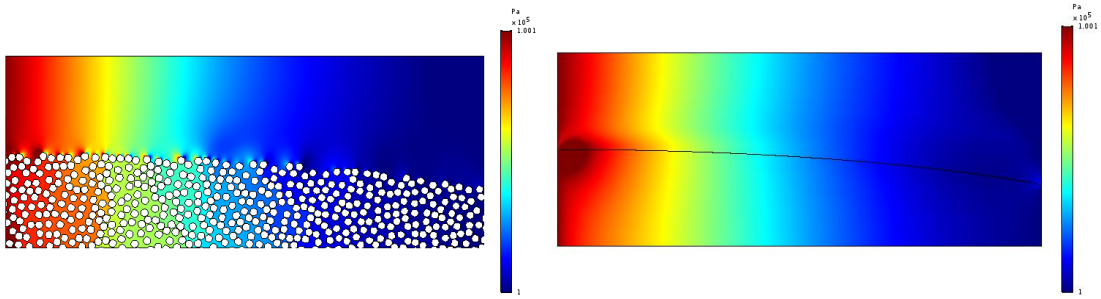

(a) Realistic model (b) CHNSD coupling model

Figure 4: Pressure distribution at time: 0.035s

In Figure **5**, pressure distributions of both realistic model and CHNSD coupling method are compared with each other. The result of coupling model meets with the realistic model very well. From the results, we can clearly see the phenomenon that pressure diffuses faster along the horizonal flow direction intra tow than inter tow. This can be explained by the porous structure cause the generation of capillary force in the tow domain which has been depicted in eq.8. Velocity fields are also explored and illustrated in Figure 5.

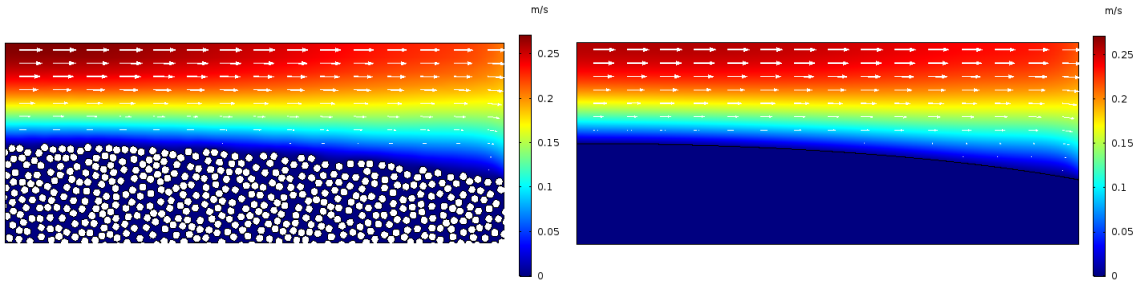

(a) Realistic model (b) CHNSD coupling model

Figure 5: Velocity field distribution at time: 0.5s

Resin flows faster inter tow than intra tow as shown in **Figure 5**. In fact, the calculated velocity intra tow domain is close to 0 m/s. A detailed plot is presented in **Figure 6** to describe the velocity distribution on a cut line of the model at the position x = 0.5 mm and the time is 0.5s.

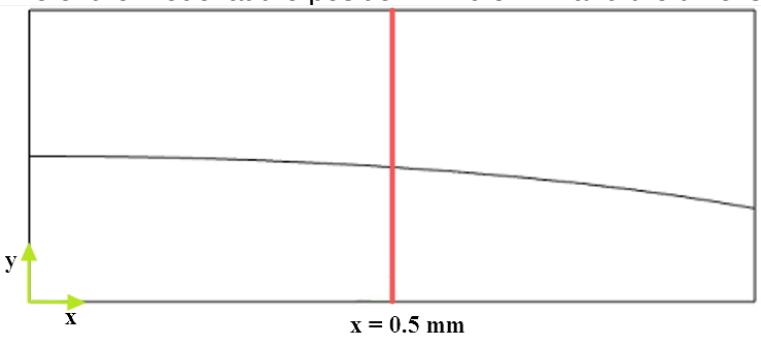

(a) Cut line location x = 0.5 mm

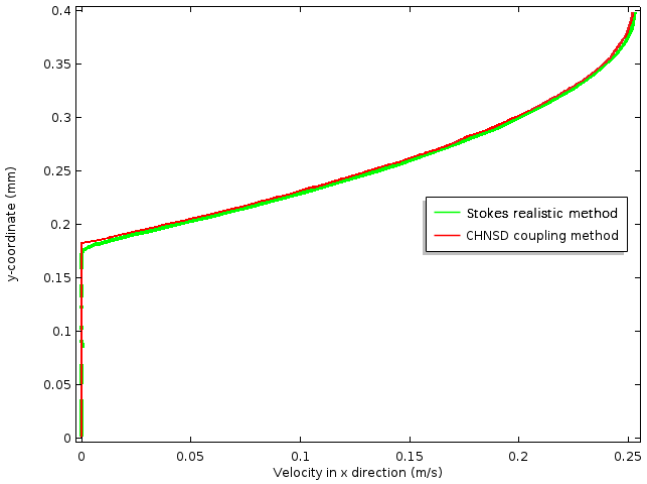

(b) Velocity distribution along the cut line at x = 0.5mm, time: 0.5s

Figure 6: Velocity distribution by both methods

As presented in Figure **6**(b), curves of velocity distribution achieved by both methods meet each other quite well. For Stokes realistic method line, there are several breaking points in the line intra tow domain since in the realistic model there are fibers at the breaking points. For both two curves intra tow domain, the velocity all along the cut line stays the same at quite low values while inter tow, the further of the position away from the tow, the higher value of the velocity it is. This appearance reveals the truth that even in the transient flow, the velocity and pressure distribution will reach and stay in a steady state after a while. Resin flow inter tow is the dominating velocity contributor in the whole impregnation process.

4. Conclusion

In this study, a model set up based on CHNSD theory is presented with extended BJS boundary condition to simulate the infusion process of LCM process at meso scale to track the flow front of the resin with the initially full of the air phase. Results of pressure, velocity and transient saturation are compared and verified with model using Stokes equation based on a realistic fiber model applied. In this model, we can conclude that with the pressure difference condition set on inlet and outlet, intra tow domain, the pressure diffuses in advance than that inter tow region at same position in x direction. In addition, the velocity perpendicular to the fiber tow intra tow maintains the same close to zero while inter tow velocity increases with the distance from the tow.

Influences of variant boundary conditions and resin or fiber reinforcement properties can be discussed on this model for next step. Numerical simulation by applying this method can be extended to macro-scale, reinforcement with anisotropic permeabilities and 3D complex geometric models in future work.

References

[1] W.R. Hwang, S.G. Advani, Numerical simulations of Stokes–Brinkman equations for permeability prediction of dual scale fibrous porous media, Physics of Fluids, 22, 113101, 2010.

[2] M. Blais, N. Moulin, P.-J. Liotier, S. Drapier, Resin infusion-based processes simulation: coupled Stokes-Darcy flows in orthotropic preforms undergoing finite strain. International Journal of Material Forming, 10 (1), 2017, pp. 43-54.

[3] Z.Q. Huang, B. Gao, X.Y. Zhang and J. Yao, On the Coupling of Two-phase Free Flow and Porous Flow, Proceeding of ECMORXIV-15th European Conference on the Mathematics of Oil Recovery, Amsterdam, Netherlands, 2016, (DOI: 10.3997/2214-4609.201601774)

[4] D. Han, D. Sun, X. Wang, Two-phase flows in karstic geometry, Mathematical Methods in the Applied Sciences, 37 (18), 2014, pp. 3048-3063.

[5] H. Xie, A. Li, Z. Huang, B. Gao, R. Peng, Coupling of two-phase flow in fractured-vuggy reservoir with filling medium. Open Physics.15 (1), 2017, (doi:https://doi.org/10.1515/phys- 2017-0002).

[6] C. Li, A. Cantarel, X. Gong, D.K. Liang, Numerical Simulation of Infusion at Microscale Permeability Calculation, Proceedings of 21th International Conference on Composite Materials 2017 (ICCM-21), X'ian, China, 2017.

[7] C. Li, A. Cantarel, X. Gong, Influence of structural parameters at microscale on the fiber reinforcement, Journal of Composite Materials, 2019;53(7):863-872.

[8] C. Li, A. Cantarel, X. Gong, A study on resin infusion and effects of reinforcement structure at dual scales by a quasi-realistic numerical simulation method. Journal of Composite Materials. 2020;54(27):4157-4171. doi:10.1177/0021998320926707

[9] C. Redondo, G. Rubio, E. Valero. On the efficiency of the IMPES method for two phase flow problems in porous media, Journal of Petroleum Science and Engineering, 164, 2018, pp. 427- 436.